NOTES AND CORRESPONDENCE

Tropical Atmospheric Variability Forced by Oceanic Internal Variability

MARKUS JOCHUM, CLARA DESER, AND ADAM PHILLIPS

National Center for Atmospheric Research, Boulder, Colorado

(Manuscript received 10 November 2005, in final form 22 May 2006)

ABSTRACT

Atmospheric general circulation model experiments are conducted to quantify the contribution of internal oceanic variability in the form of tropical instability waves (TIWs) to interannual wind and rainfall variability in the tropical Pacific. It is found that in the tropical Pacific, along the equator, and near 25°N and 25°S, TIWs force a significant increase in wind and rainfall variability from interseasonal to interannual time scales. Because of the stochastic nature of TIWs, this means that climate models that do not take them into account will underestimate the strength and number of extreme events and may overestimate forecast capability.

1. Introduction

This study is part of a series of studies aimed at quantifying the effect of tropical instability waves (TIWs) in the ocean on tropical climate. Caused by instabilities of the zonal equatorial ocean currents, TIWs have a period between 20 and 40 days, and on these time scales they cause variability in SST (Legeckis 1977), cloud cover (Deser et al. 1993), and wind (Chelton et al. 2001; Hashizume et al. 2001; Small et al. 2003). Unlike linear planetary waves, TIWs make a net contribution to the equatorial heat budget because they not only move heat horizontally toward the equator (Hansen and Paul 1984) but also increase vertical mixing in the upper ocean and thereby the atmosphere–ocean heat flux (Jochum et al. 2005; Jochum and Murtugudde 2006). Mixing is an irreversible process and therefore TIWs pump heat from the equatorial mixed layer into the thermocline. Thus, SST in the eastern and central Pacific depends, among other things, on the level of TIW activity. An important finding for the present study is that TIWs are nonlinear and therefore vary in strength from year to year even under climatological forcing (Jochum et al. 2004a). This nonlinearity combined with their importance to the equatorial heat budget led to the hypothesis that a part of the observed interannual variability in SST can be explained by the stochastic nature of TIWs. A series of studies then showed that, indeed, in the central Atlantic, eastern Pacific, and western Indian Ocean, approximately one-third of the observed interannual SST variability is due to instability waves (Jochum et al. 2004b; Jochum and Murtugudde 2004, 2005).

The purpose of the present study is to investigate whether the stochastic nature of TIWs increases the variability of the tropical atmosphere on interseasonal–interannual time scales. The "forced-ocean" studies cited above could only speculate that internally generated equatorial SST variabilities cause tropical climate variability by, for example, modifying the seasonal cycle of the Pacific and Atlantic intertropical convergence zone (ITCZ) or the Indian Ocean monsoon. Here it will be shown that these internally generated SST variabilities are indeed large enough to create significant wind and rainfall anomalies over the equatorial Pacific. To quantify the magnitude by which oceanic internal variability increases atmospheric variability, we compare the results from two identical AGCMs, one forced with climatological SSTs and the other forced with the same SST plus the interseasonal–interannual component of the SST variability created by TIWs. It is important to note that the effect of individual TIWs on SST variability is *not* addressed here;

Corresponding author address: Dr. Markus Jochum, National Center for Atmospheric Research, P.O. Box 3000, Boulder, CO 80307.
E-mail: markus@ucar.edu

DOI: 10.1175/JCLI4044.1

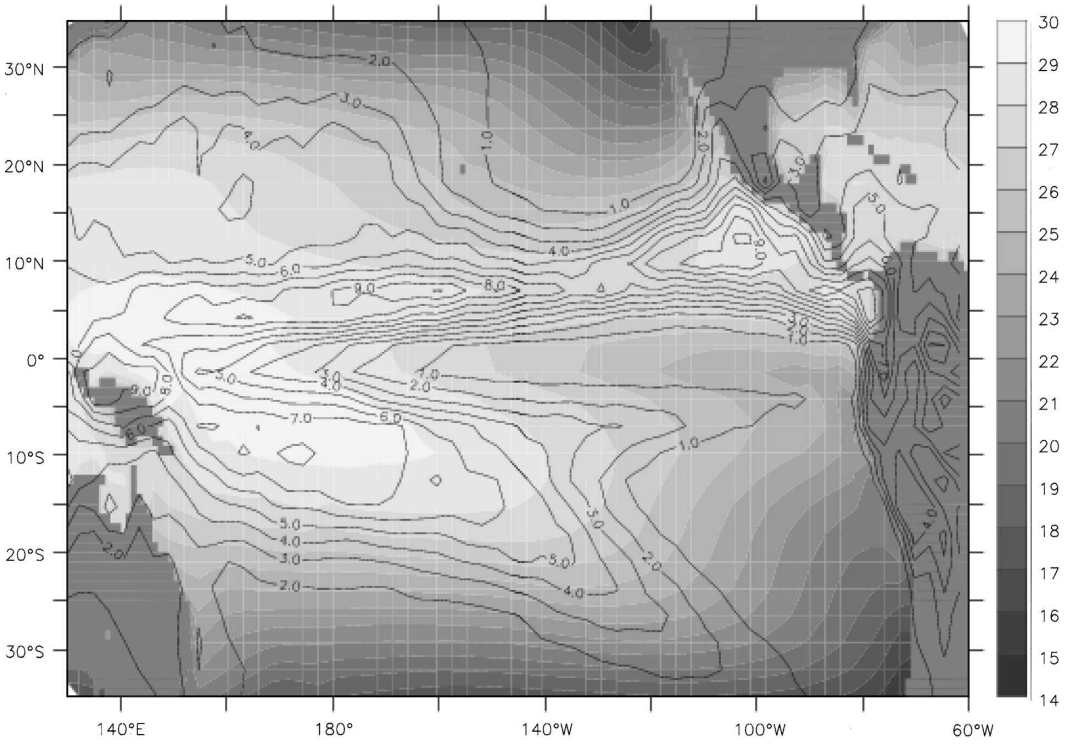

FIG. 1. Climatology of observed tropical Pacific SST (shaded) and rainfall (contour interval: 1 mm day^{-1}) simulated from a 25-yr integration of CAM3 forced with observed monthly SST climatology.

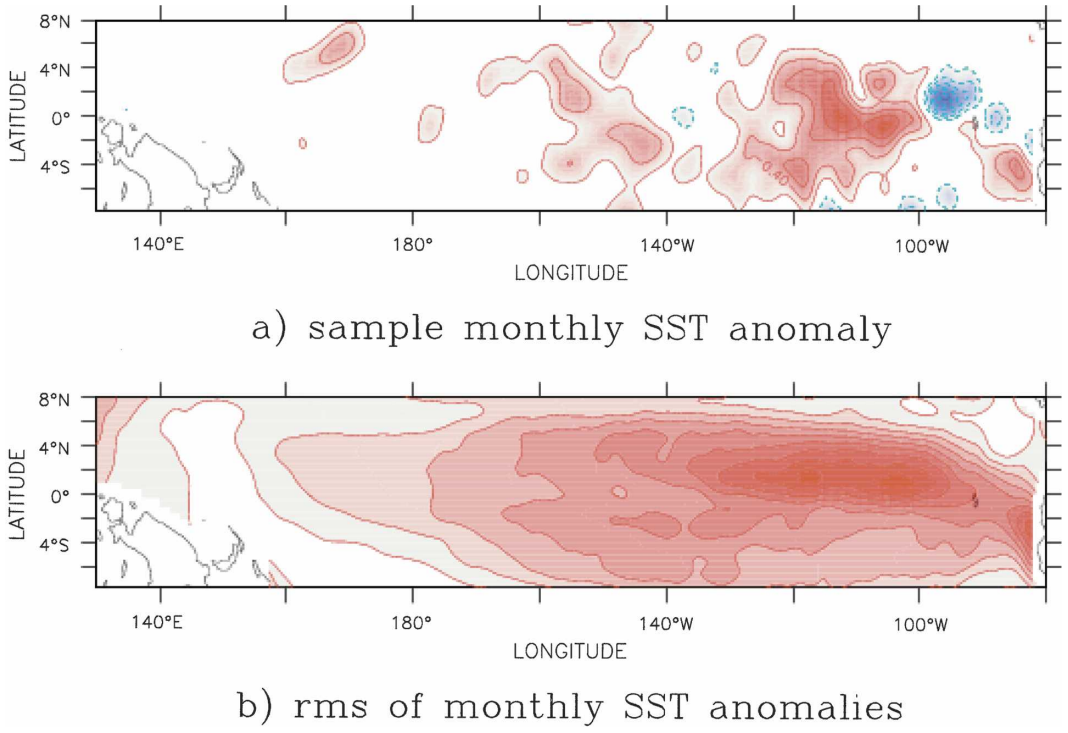

FIG. 2. Visualization of the SST anomaly field used in experiment TIW. (a) A sample monthly SST anomaly field illustrates the spatial scales (contour lines: 0.2°C) and (b) the amplitude and the geographical distribution of the signal is described by the rms of the SST anomaly field (contour lines: 0.05°C; maximum value: 0.5°C). During the particular July shown in (a), the equatorial Pacific is warmer than usual over a large part of the eastern basin. For details see Jochum and Murtugudde (2004).

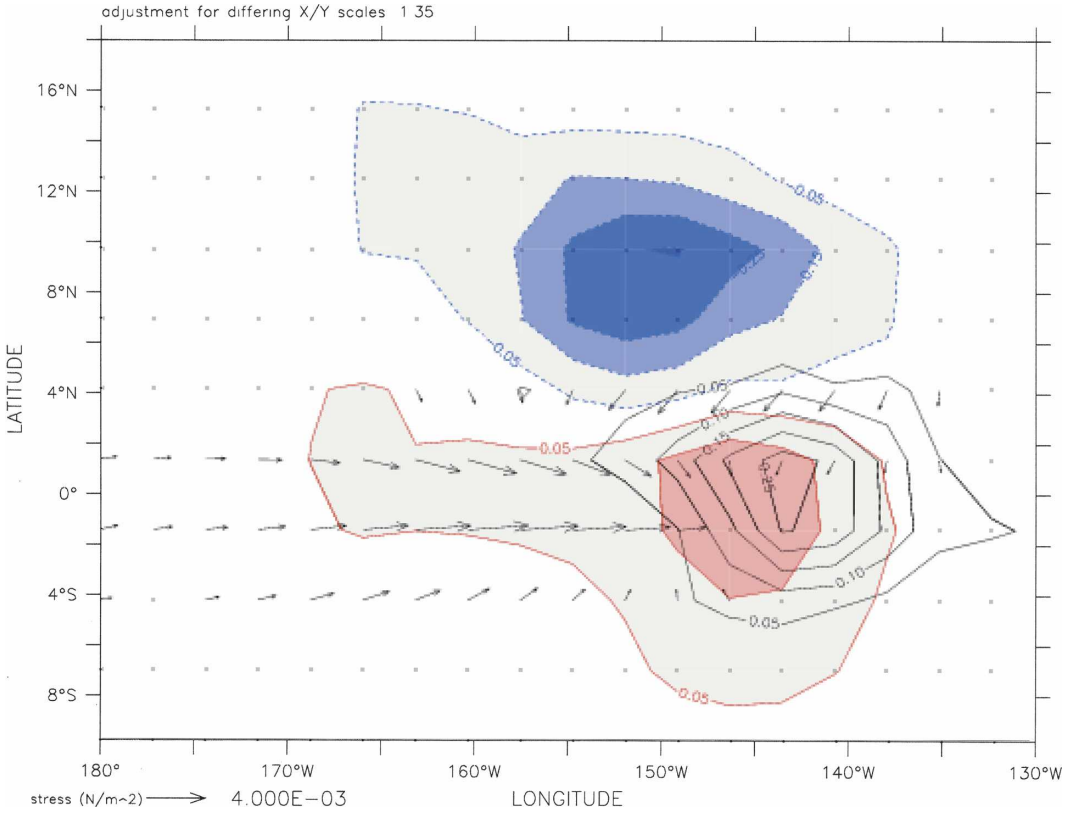

FIG. 3. Regression of SST, precipitation, and wind stress anomalies onto the SST anomaly averaged between 3°S–3°N and 145°–139°W. Only the statistically significant regressions are shown [correlation coefficient of at least 0.15 for a 95% confidence interval; the contour interval for precipitation is 0.1 mm day^{-1} (color) and for SST is 0.05°C (black)]. Thus, an SST anomaly of 0.25° (approximately the TIW-induced rms of SST; see Fig. 2) in this area will at 8°N, 150°W reduce the rainfall rate by 0.3 mm day^{-1} and reduce the easterlies at 1°S, 160°W by 0.004 N m^{-2}. Regressions for SST anomalies farther west and east are smaller because toward the west TIWs are weaker and toward the east the mean SST is colder (and convection is less sensitive to SST changes).

rather, the present experimental design isolates the nonlinear rectification effect of TIWs and only allows statements about interseasonal–interannual variability.

The next section describes the experiments, section 3 quantifies the impact of oceanic internal variability on the atmosphere, and the last section summarizes the results.

2. The experiments

We analyze the output of two forced AGCM runs. In both runs the model is identical—version 3 of the Community Atmospheric Model (CAM3) from the National Center for Atmospheric Research (NCAR) in its T42 configuration. It is a spectral model with 26 layers and a horizontal resolution of approximately 2.8°. It contains state-of-the-art treatments of convection and clouds. Details can be found in Collins et al. (2006).

The two experiments are integrated for 25 yr and differ in their SST forcing only. The control experiment (CON) is forced with the monthly climatology of Hurrell et al. (2005, unpublished manuscript; Fig. 1 of the current paper), and the TIW experiment (TIW) is forced with the sum of the monthly climatology and a monthly SST anomaly field taken from the eddy-resolving tropical Pacific Ocean simulation described in Jochum and Murtugudde (2004). This eddy-resolving simulation was forced with a climatological seasonal cycle of atmospheric fluxes, so any deviation from the model's climatological seasonal cycle is due to TIWs (Jochum et al. 2004b). The anomaly field consists of 25 yr (years 21–45 of the 60-yr integration of Jochum and Murtugudde 2004) of deviations from the monthly climatological values at every grid point. It is restricted to the Pacific Ocean between 10°S and 10°N. By construction, the long-term mean of the anomaly is zero at every grid point. It is important to note that the anomalies are averaged over one month and regridded onto the T42

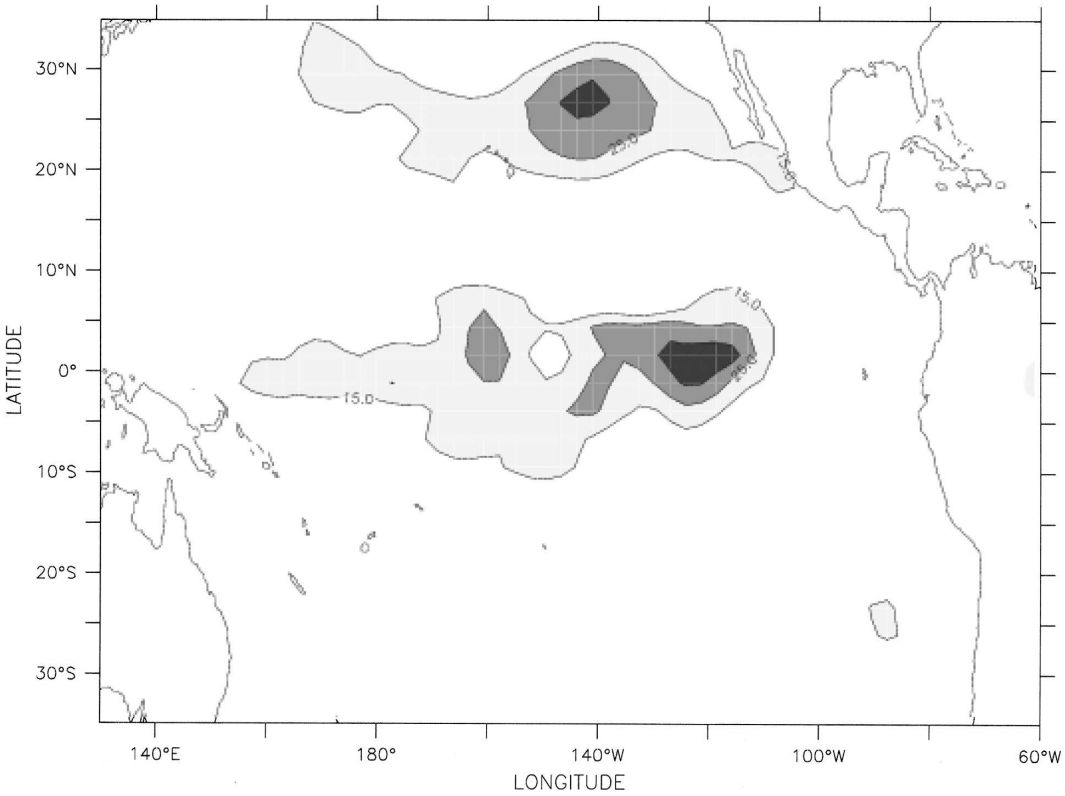

FIG. 4. Difference in the rms of the noise in the zonal wind stress between TIW and CON [in percent; only the statistically significant (95%) differences are shown; contour interval is 10%; the largest value is 35%]. The pattern is similar for the meridional wind stress (not shown).

grid of the AGCM. Thus, the AGCM does not see the individual TIWs but only the large-scale nonlinear rectification effect of more or less TIW activity (see introduction). The monthly SST anomaly field is illustrated in Fig. 2.

Note that the experimental design and hypothesis are very different from the ones in Small et al. (2003). Small et al. (2003) analyzed the direct impact that individual TIWs have on the planetary boundary layer by forcing a high-resolution AGCM with an SST field that was highly resolved in time and space. Here the focus is on the effect that varying TIW activity has on the longer-term variability of the tropical atmosphere. Small et al. (2003) addresses one possible forcing mechanism for atmospheric *intra*seasonal variability; the present study addresses one possible forcing mechanism for atmospheric *inter*seasonal–interannual variability.

The experimental design makes the implict assumption that on eddy time scales, the atmospheric response does not amplify or weaken the eddies. Idealized studies by Pezzi et al. (2004) and recent high-resolution coupled GCM studies by H. Seo (2005, personal communication) suggest that this is a reasonable assumption. One could imagine an alternative experimental setup in which both the atmosphere and the ocean model fully resolve the eddies. However, the costs for such an experiment would be prohibitive and the technical difficulties of damping the eddies without affecting anything else in the model are quite challenging if not impossible to overcome.

3. Atmospheric response

The autocorrelation length and time scales of the rectified monthly SST anomalies associated with TIWs are approximately 1000 km (Fig. 2) and 2 months (not shown), respectively. This is large and long enough to generate a balanced, planetary wave response in the tropical atmosphere (Gill 1980). The analyses of wind and rainfall anomalies and rectified TIW-induced SST anomalies reveal that the response is indeed what is expected from a linear atmospheric response to localized equatorial heating anomalies (see Gill 1980, his Fig. 1a): the air flows toward the warmer SST, and the resulting southward shift of the ITCZ leads to increased rainfall on the equator and reduces convergence and rainfall to the north of it (Fig. 3). Note that the atmospheric response depends not only on the level of TIW

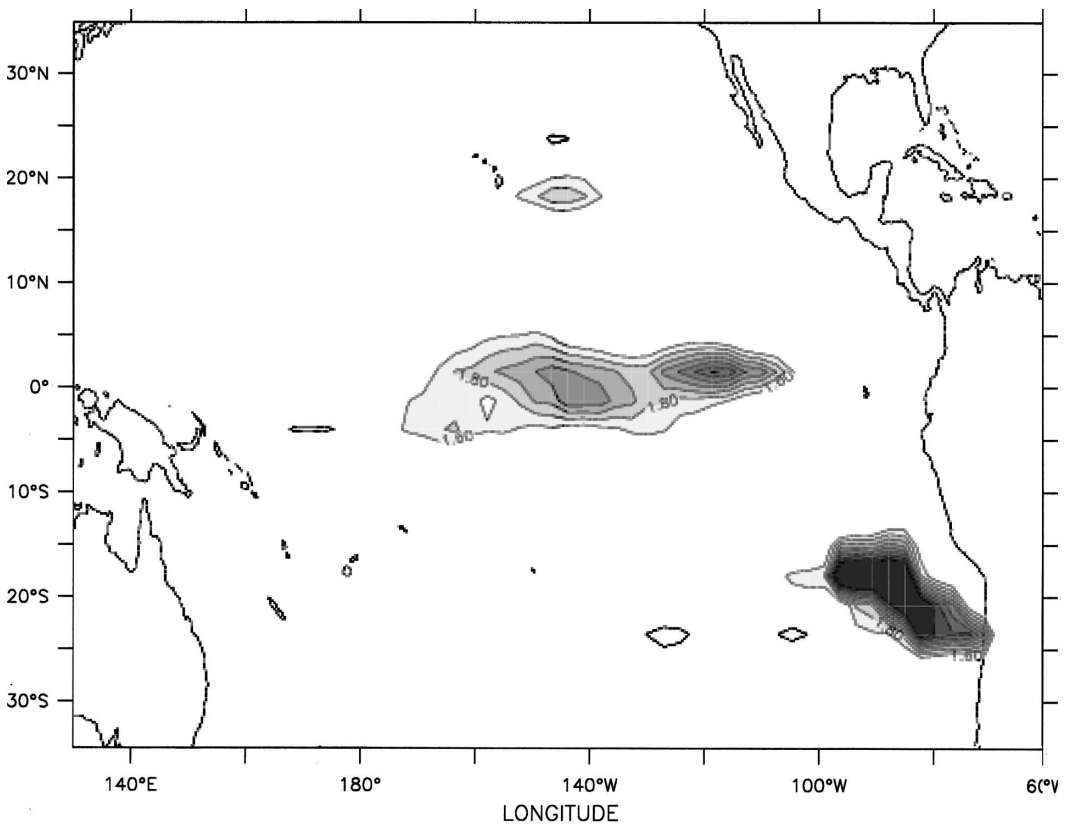

FIG. 5. Ratio of the rms of the annual rainfall maxima between TIW and CON [only statistically significant (95%) values are shown; contour interval is 0.2; the largest equatorial value is 2.8]. For example, in the central equatorial Pacific, the rms of the rainfall maximum (rainfall in a year's most rainy month) is about twice as large in TIW as in CON.

activity but also on the background SST. The maximum response is found for anomalies between 150° and 140°W; the response is limited by cooler background SST east of this region and by reduced TIW activity west of this region. In the rest of this section, we investigate how large this atmospheric response to SST anomalies is compared to the internal atmospheric variability in CON.

In quantifying the atmospheric response to the stochastic component of TIWs, we limit ourselves to rainfall and wind stress—wind stress because it has direct implications for the behavior of the coupled system and rainfall because it presents a vertical integral of changes throughout the atmosphere and is also of societal relevance. The mean and seasonal cycles of both variables are indistinguishable within the uncertainty (not shown), therefore we will only discuss the deviations from the climatologies of CON and TIW. In both experiments, the variance of these deviations (hereafter noise) is red for periods of approximately 100 days and shorter and white for longer periods [not shown; see Frankignoul and Hasselmann (1977) for a discussion on stochastic climate models]. However, as shown below, in some areas the noise is significantly larger in TIW than in CON. This is a key result of the present study.

As expected, the zonal wind variability increases along the equator where the SST anomalies are imposed (Fig. 4). There is also a secondary maximum along 25°N (Fig. 4) that we speculate is caused by atmospheric teleconnections as described in Trenberth et al. (1998). However, the detailed dynamics of the atmospheric teleconnections are beyond the scope of this study; the important result is that TIWs increase the variability on interseasonal and longer time scales.

The pattern and relative magnitude of the increase in rainfall variability between TIW and CON is similar to that for wind (not shown), so instead the variability of maximum monthly rainfall will be shown here. Because the rainfall maximum occurs in different months at different locations, the variability was computed for the rainiest month at every grid point (e.g., February for 20°N, 150°W, April for 0°, 140°W, June for 20°S, 90°W, etc.). The variability of the rainfall maxima increases significantly not only along the central equatorial Pa-

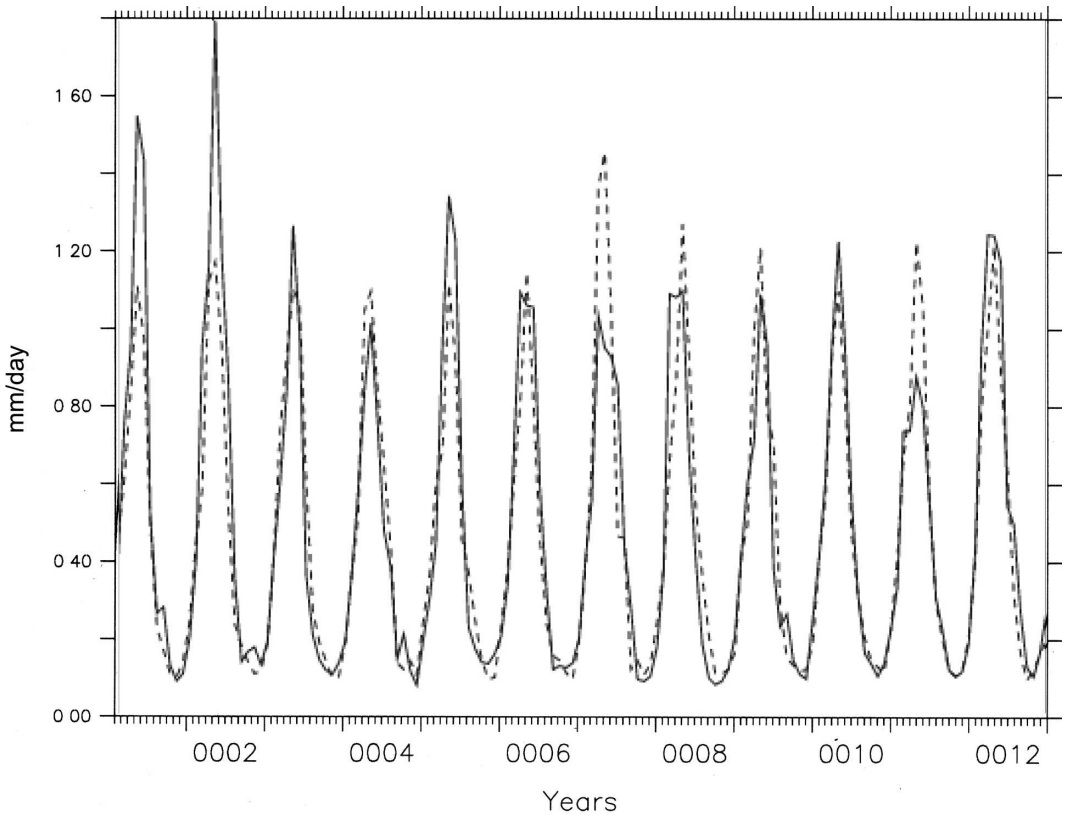

FIG. 6. Rainfall averaged over 3°S–3°N and 150°–100°W for CON (broken line) and TIW (solid line); for better visibility, only the first 12 yr are shown. While in CON the maximum rainfall stays in a narrow range around 1.2 mm day^{-1}, TIW creates extreme maxima (e.g., yr 2) and minima (e.g., yr 11).

cific but also near 20°N, 150°W and 20S°, 90°W (Fig. 5). The equatorial maximum reaches into the northern ITCZ and the western Pacific warm pool (recall Fig. 1). This leads not only to relative extrema but also to large absolute anomalies. For example, in TIW, the April rainfall averaged over the eastern Pacific ranges from 0.9 to 1.8 mm yr^{-1}, whereas in CON the range is much less (Fig. 6).

4. Summary and discussion

Intraseasonal eddies in the equatorial oceans are nonlinear. Therefore their strength varies from year to year, even under climatological forcing. Since they make a substantial contribution to the mixed layer heat budget, they cause interseasonal–interannual variability of SST. Here it was shown that in the equatorial Pacific, these SST anomalies are large enough to increase the atmospheric variability in rainfall and wind stress. Thus, intraseasonal equatorial eddies force interseasonal–interannual equatorial climate variability.

This result comes with the caveat that it is a modeling study. It will not be possible to quantify this nonlinear rectification effect with observations, so the present results are only as trustworthy as the model's individual components. Both the AGCM and the OGCM used in the present study are state-of-the-art models, and the results agree qualitatively with the expectations from theory [cf. Fig. 1 of Gill (1980); Fig. 3 of the current paper]. Therefore the process itself cannot be argued; only its magnitude can. In the present model, the wind anomalies have an autocorrelation length of approximately 2000 km and their rms is approximately 10% of the zonal mean wind stress. Thus, east of the date line, the noise due to TIWs is similar to that created by the Madden–Julian oscillation (MJO; Waliser et al. 2003, 2004). The same is also true for the rectified SST anomalies, as already pointed out by Jochum and Murtugudde (2004). To be clear, the MJO-induced variability in the western Pacific is larger than the TIW-induced variability anywhere, but the TIWs provide an additional mechanism to create atmospheric variability that acts in a different region than the MJO.

The present results have one important implication:

coupled climate models that do not resolve equatorial ocean eddies will underestimate climate variability on all time scales, will not give an adequate representation of extreme events, and will overestimate their forecast capability. This could explain, for example, why current climate models commonly lack tropical intraseasonal variability (Deser et al. 2006; Lin et al. 2006). A recent study by Roberts et al. (2004) suggests that resolving oceanic eddies in coupled GCMs does indeed improve the variability of SST. It should be pointed out that after minor adjustments to the horizontal viscosity scheme, the NCAR ocean model realistically represents TIWs. This suggests that other GCMs, many of which also use a resolution in the equatorial ocean of approximately $1^\circ \times 1/3^\circ$, should be able to generate TIWs as well. Therefore, the increased and improved atmospheric variability in GCMs would come at no additional computational costs.

Acknowledgments. This research was supported by NSF through NCAR and by NOAA funds for mesoscale air–sea interaction. The authors are grateful to Raghu Murtugudde for many discussions and to Bill Large for his enthusiasm.

REFERENCES

Chelton, D. B., and Coauthors, 2001: Observations of coupling between surface wind stress and sea surface temperature in the eastern tropical Pacific. *J. Climate,* **14,** 1479–1498.

Collins, W. D., and Coauthors, 2006: The Community Climate System Model version 3 (CCSM3). *J. Climate,* **19,** 2122–2143.

Deser, C., S. Wahl, and J. J. Bates, 1993: The influence of sea surface temperature gradients on stratiform cloudiness along the equatorial front in the Pacific Ocean. *J. Climate,* **6,** 1172–1180.

——, A. Capotondi, R. Saravanan, and A. Phillips, 2006: Tropical Pacific and Atlantic climate variability in CCSM3. *J. Climate,* **19,** 2451–2481.

Frankignoul, C., and K. Hasselmann, 1977: Stochastic climate models and their application to SST anomalies and thermocline variability. *Tellus,* **29,** 289–305.

Gill, A., 1980: Some simple solutions for heat-induced tropical circulation. *Quart. J. Roy. Meteor. Soc.,* **106,** 447–462.

Hansen, D., and C. Paul, 1984: Genesis and effects of long waves in the equatorial Pacific. *J. Geophys. Res.,* **89,** 10 431–10 440.

Hashizume, H., S. Xie, T. Liu, and K. Takeuchi, 2001: Local and remote atmospheric response due to tropical instability waves: A global view from space. *J. Geophys. Res.,* **106,** 10 173–10 185.

Jochum, M., and R. Murtugudde, 2004: Internal variability in the tropical Pacific Ocean. *Geophys. Res. Lett.,* **31,** L14309, doi:10.1029/2004GL020488.

——, and ——, 2005: Internal variability of Indian Ocean SST. *J. Climate,* **18,** 3726–3738.

——, and ——, 2006: Temperature advection by tropical instability waves. *J. Phys. Oceanogr.,* **36,** 592–605.

——, P. Malanotte-Rizzoli, and A. Busalacchi, 2004a: Tropical instability waves in the Atlantic Ocean. *Ocean Modell.,* **7,** 145–163.

——, R. Murtugudde, P. Malanotte-Rizzoli, and A. Busalacchi, 2004b: Internal variability in the Atlantic Ocean. *Ocean–Atmosphere Interaction and Climate Variability, Geophys. Monogr.,* Vol. 147, Amer. Geophys. Union, 181–187.

——, ——, R. Ferrari, and P. Malanotte-Rizzoli, 2005: The impact of horizontal resolution on the equatorial mixed layer heat budget in ocean general circulation models. *J. Climate,* **18,** 841–851.

Legeckis, R., 1977: Long waves in the eastern equatorial Pacific Ocean: A view from a geostationary satellite. *Science,* **197,** 1179–1181.

Lin, J.-L., and Coauthors, 2006: Tropical intraseasonal variability in 14 IPCC AR4 climate models. Part I: Convective signals. *J. Climate,* **19,** 2665–2690.

Pezzi, L. P., J. Vialard, K. J. Richards, C. Menkes, and D. Anderson, 2004: Influence of ocean–atmosphere coupling on the properties of tropical instability waves. *Geophys. Res. Lett.,* **31,** L16306, doi:10.1029/2004GL019995.

Roberts, M. J., and Coauthors, 2004: Impact of an eddy-permitting ocean resolution on control and climate change simulations with a global coupled GCM. *J. Climate,* **17,** 3–20.

Small, J., S.-P. Xie, and Y. Wang, 2003: Numerical simulation of atmospheric response to Pacific tropical instability waves. *J. Climate,* **16,** 3722–3740.

Trenberth, K. E., G. W. Branstator, D. Karoly, N. Lau, and C. Ropelewski, 1998: Progress during TOGA in understanding and modeling global teleconnections associated with tropical sea surface temperatures. *J. Geophys. Res.,* **103,** 14 291–14 324.

Waliser, D. E., R. Murtugudde, and L. E. Lucas, 2003: Indo-Pacific Ocean response to atmospheric intraseasonal variability: 1. Austral summer and the Madden–Julian Oscillation. *J. Geophys. Res.,* **108,** 3160, doi:10.1029/2002JC001620.

——, ——, and ——, 2004: Indo-Pacific Ocean response to atmospheric intraseasonal variabilty: 2. Boreal summer and the intraseasonal oscillation. *J. Geophys. Res.,* **109,** C03030, doi:10.1029/2003JC002002.